Front. Environ. Sci. Eng. 2016, 10(2): 211–218
DOI 10.1007/s11783-014-0753-y

RESEARCH ARTICLE

Effective degradation of tetracycline by mesoporous Bi_2WO_6 under visible light irradiation

Xiaolong CHU, Guoqiang SHAN, Chun CHANG, Yu FU, Longfei YUE, Lingyan ZHU (✉)

College of Environmental Science and Engineering, Nankai University, Tianjin 300071, China

Abstract Bi_2WO_6 was synthesized with a hydrothermal method at different pHs and used for the degradation of tetracycline (TC) in water. The mesoporous Bi_2WO_6 prepared at pH 1 (BWO-1) displayed the highest adsorption and degradation capacity to TC due to its large surface area and more efficient capacity to separate photogenerated electrons and holes. 97% of TC at 20 mg $\cdot L^{-1}$ was removed by BWO-1 at 0.5 g$\cdot L^{-1}$ after 120 min irradiation under simulated solar light. Only 31% of the total organic carbon (TOC) was removed after 360 min irradiation although the TC removal reached 100%, suggesting that TC was mainly transformed to intermediate products rather than completely mineralized. The intermediates were identified by high-performance liquid chromatography-time of flight-mass spectrometry (HPLC-TOF-MS) and possible photodegradation pathways were proposed.

Keywords Bi_2WO_6, hydrothermal synthesis, tetracycline (TC), photocatalysis

1 Introduction

Antibiotics have been widely used in human and veterinary medicines for several decades [1]. Due to their poor absorption efficiency, most of them are excreted through feces and urine as un-metabolized parent compounds [2]. As a result, antibiotics are widely present in municipal wastewater and surface water. Their presence in surface water could result in adverse effects to aquatic organisms and ecological system. However, they cannot be removed by traditional wastewater treatment techniques [1–4].

Among all the antibiotics, tetracycline (TC) is one of the most used in aquaculture and veterinary medicines. Large amount of TC has been detected in sewage water (0.1 – 1.0 $\mu g \cdot L^{-1}$) [5,6], surface water (0.11 $\mu g \cdot L^{-1}$ in the United States [7], 4.2 $\mu g \cdot L^{-1}$ in Germany [8]), groundwater and even in drinking water [9,10]. Several methods have been developed to eliminate TC in aqueous solution, including ozonation degradation [11], photo-electro-Fenton oxidation [12], ultraviolet radiation [13], photocatalytic degradation [14,15], and etc. In recent years, photocatalysis for TC degradation using semiconductor catalysts has become a cost-effective and environmentally sustainable treatment method.

The most widely used photocatalyst is TiO_2. Zhu et al. [14] used nanosized TiO_2 to degrade TC in water under UV irradiation, and 95% of TC was eliminated after 60 min irradiation. However TiO_2 can only been excited by ultraviolet light shorter than 387.5 nm, which only accounts for about 4% of the sunlight [16]. In addition, it is easy for the photo-generated electrons and holes in TiO_2 to recombine due to its morphology and properties [17]. Recently, many new photocatalysts such as Bi_2WO_6 [18,19], $BiVO_4$ [20], which were first discovered by Kudo et al. in the late 1990's [21], have been developed to overcome the drawbacks of TiO_2. The most important characteristic of these new photocatalysts is that they display high photocatalytic activity under visible light. Among these photocatalysts, Bi_2WO_6 has attracted considerable attention. It can induce effective separation of photo-generated electron-hole pairs and achieve a high photocatalytic performance, owing to its unique layered-structure. Wang et al. [22] reported that Bi_2WO_6 prepared at pH 11 displayed very efficient photodegradation capacity to bisphenol A (BPA) under simulated solar light. Chen et al. [23] discovered that Bi_2WO_6 could degrade Microcystin-RR (MC-RR) efficiently under near ultraviolet light.

The objective of this study was to investigate the degradation of TC in water using Bi_2WO_6 as photocatalyst under simulated solar light irradiation. We used Bi_2WO_6 to degradate tetracycline for the first time. Bi_2WO_6 was synthesized using hydrothermal method with pH varying in the range of 1 – 11. The synthesized catalysts were characterized by means of a variety of analytical methods.

Received May 26, 2014; accepted September 21, 2014

E-mail: zhuly@nankai.edu.cn

The possible photocatalytic mechanisms were also investigated based on the information of the produced intermediates.

2 Materials and methods

2.1 Materials and chemical

$Bi(NO_3)_3 \cdot 5H_2O$, $Na_2WO_4 \cdot 2H_2O$, NaOH, $(NH_4)_2C_2O_4$, HNO_3 and glacial acetic acid (analytical grade) were purchased from Chemical Technology Co., Ltd., Tianjin, China. Tetracycline (TC) was purchased from Sigma–Aldrich (Shanghai, China) and was of chromatographic grade. *N,O*-bis (trimethylsilyl) trifluoroacetamide (BSTFA) was purchased from J&K chemical company, USA. Methanol of high performance liquid chromatography (HPLC) grade used for the mobile phase was purchased from Concord Technology Co., Ltd., Tianjin, China. Formic acid (HPLC grade) used for liquid chromatography coupled with mass spectrometer (LC-MS) analysis were purchased from Dikma Technology Inc., USA.

2.2 Preparation and characterization of Bi_2WO_6

Bi_2WO_6 was prepared using the hydrothermal method described by Wang et al. [22]. 20 mL of sodium tungstate solution at 0.10 $mol \cdot L^{-1}$ was mixed with 20 mL of bismuth nitrate solution at 0.20 $mol \cdot L^{-1}$. The mixed solution was vigorously stirred and ultrasonicated at room temperature for 30 min sequentially. The pH of the reaction solution was adjusted with diluted HNO_3 or NaOH solution to 1.0, 4.0, 7.0, 9.0 and 11.0, respectively. The as-prepared catalysts were denoted as BWO-1, -4, -7, -9, and -11, respectively. The suspension was transferred to a 40 mL Teflon-lined autoclave and then heated to 140°C for 20 h in an oven. The precipitates were collected by centrifugation, washed with water and ethanol for three times and dried at 120 °C for 6 h. The X-ray diffraction (XRD) was carried on a D/MAX 2500 V diffractometer (Rigaku, Japan) using monochromatized Cu Kα radiation under 40 kV and 100 mA and the scanning range was from 20° to 80°. Field Emission Scanning Electron Microscope (1530VP, phoenix-dx 60 s, OIM, Germany) provided the morphology of the photocatalysts. UV-vis diffuse reflectance spectra were recorded using a Hitachi U-3010 spectrometer in the range of 200–600 nm. Brunauer-Emmett-Teller (BET) surface area and pore size measurements were performed on an autosorb-1-MP 1530VP automatic surface area and pore size analyzer. Photoelectrochemical test with an Autolab PGSTAT302N electrochemical system (Metrohm Ltd., Switzerland) was carried out in a conventional three-electrodes, a single-compartment quart cell filled with 0.1 $mol \cdot L^{-1}$ Na_2SO_4 electrolyte and a potentiostat. The working electrode was the ITO/photocatalyst electrode. A platinum wire was used as a counter electrode with Ag/AgCl (saturates KCl) as a reference electrode. We switched on and off to measure the photoresponses of the photocatalysts under visible light ($\lambda > 400$ nm) at 0.0 V. Electrochemical impedance spectra (EIS) were recorded at 0.0 V. A sinusoidal ac perturbation of 10 mV was applied to the electrode over the frequency range of 0.01–10^4 Hz.

2.3 Photocatalytic reactions and analysis

The photochemical reactor (XPA-7, Nanjing, Xujiang Company, China) equipped with a 350W Xe lamp as light source, was used for the degradation of TC. The initial conditions of all photocatalytic reactions were the same: 20 mL of TC solution (20 $mg \cdot L^{-1}$) was mixed with 10 mg catalyst with constant magnetic stirring. Before illumination, the TC solution with catalysts was magnetically stirred in the dark for 30 min to establish adsorption equilibrium of TC on the catalysts. Throughout the reaction, the concentration of TC in the solution was analyzed by a high performance liquid chromatography (HPLC, Agilent 1200) with the UV detector at 355 nm wavelength. The analytical conditions were as follows: Agilent Eclipse XDB-C18 column (5 μm, 150 mm × 4.6 mm); the mobile phase was 55:45 (v/v) methanol and 0.025% glacial acetic acid aqueous solution; flow rate was set as 1 $mL \cdot min^{-1}$. After reaction, the catalysts were collected and extracted in a 20 mL mixed solution of water (50%) and methanol (50%), and then stirred for 24 h. The supernatant was analyzed for TC using HPLC to determine the amount of TC remaining on the photocatalyst. High-performance liquid chromatography coupled with time of flight-mass spectrometry (ESI-Q-TOF-MS/MS) (LC-MS/MS, Waters 2695XE, USA) and gas chromatography coupled with mass spectrometry (GC-MS, Agilent 5975GC-7890MS, USA) were used to identify the major intermediates in the reaction solution. For LC-MS, the ion mode was set on positive mode and ion scanning range was *m/z* 50–800. Before GC-MS analysis, the samples should be derivatized. Forty ml of reaction solution (the solutions in two parallel tests were combined) was centrifuged to remove photocatalysts and adjusted to pH 2.5 with 10% HCl, extracted with 15 mL of dichloromethane for three times and then dehydrated using anhydrous sodium sulfate. Afterwards, the dehydrated samples were blown down to 1 mL under a nitrogen stream. 0.5 mL of *N,O*-bis (trimethylsilyl) trifluoroacetamide (BSTFA) was added and the mixed solution was kept at 50°C for 30 min. 1 μL of the solution was injected into GC (equipped with Thermal TR-5 column).

3 Results and discussion

3.1 Characterization of the prepared catalysts

The powder X-ray diffraction (XRD) patterns which provide crystal structure and phase information of the as-

synthesized samples are displayed in Fig. 1. The diffraction peaks of the Bi_2WO_6 catalysts prepared at pH 1, 4, 7, 9 were consistent with those of russellite Bi_2WO_6 [22–24]. This agrees with the result reported by Wang et al. [22]. However the catalyst prepared at pH 11 was a mixture of Bi_2WO_6 [JCPDS NO. 39-0256] and $Bi_{3.84}W_{0.16}O_{6.24}$ [JCPDS No. 43-0447] [22,23]. Thus, BWO-11 was not discussed anymore. The solution pH may affect the solubility of WO_4^{2-} and $[Bi_2O_2]^{2+}$ and finally leads to the formation of different phases of bismuth tungsten oxide [25]. The morphology of the as-prepared photocatalysts was investigated by the SEM (Fig. S1). From the images, it can be seen clearly that Bi_2WO_6 was present as a flower-like spherical structure when the pH was in the range of 1–4. The crystallite size was about 4–10 nm thickness and mostly 200–300 nm in length. As pH increased to 7–9, the catalysts were in irregular sheet structure. The N_2 adsorption/desorption isotherm and the pore size distribution (inset) of the catalyst prepared at pH 1 are shown in Fig. S2. The isotherm was identified as type IV, which is characteristic of mesoporous structure [17,26,27]. Most of the pores in the catalyst were less than 5 nm. The catalyst displayed a nanoporous structure which was supported by the relatively large surface area and total pore volume. The S_{BET}s of the catalysts BWO-1, -4, -7, and -9 were 32.41, 26.84, 12.30 and 7.35 $m^2 \cdot g^{-1}$, respectively. The UV-vis DRS patterns of the catalysts prepared at different pH values are illustrated in Fig. 2. All the catalysts demonstrated high photoabsorption capacity in the range of UV to visible light around 450 nm, suggesting their potential photocatalytic activity under visible light. The bandgap was calculated with the formula of $E_g = 1240/\lambda_0$, where E_g and λ_0 represent bandgap and absorption edge, respectively. The bandgap was estimated to be 2.76, 2.73, 2.64 and 2.79 eV for BWO-1, -4, -7 and -9, respectively.

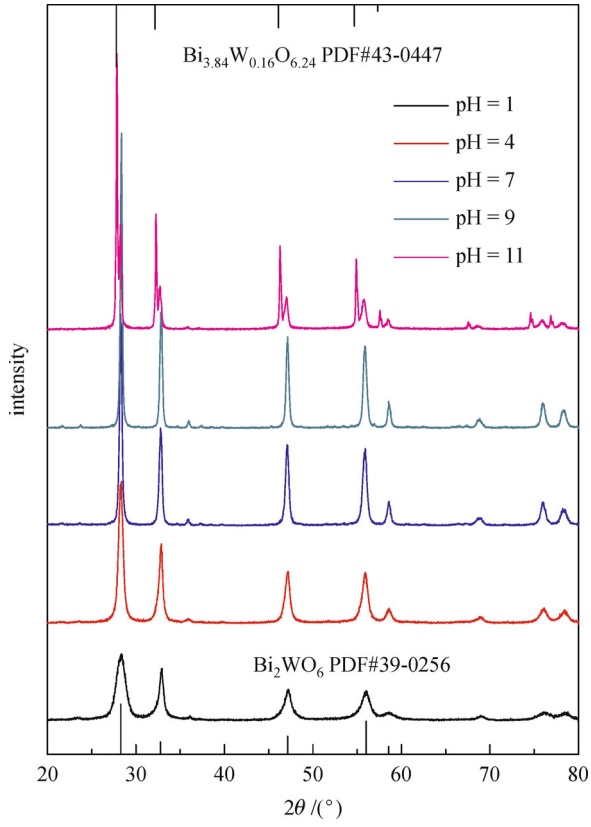

Fig. 1 XRD patterns of Bi_2WO_6 prepared at different hydrothermal pHs

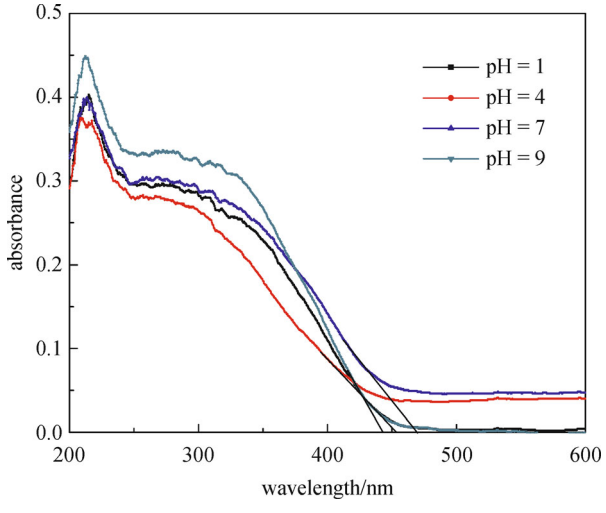

Fig. 2 Diffuse reflectance UVvis spectra of Bi_2WO_6 catalysts prepared at different hydrothermal pHs

3.2 Degradation efficiency of TC by Bi_2WO_6 prepared at different pHs

Before irradiation, TC was allowed to adsorb on the catalysts in dark for 30 min to establish adsorption equilibrium, and the sorption kinetics are shown in Fig. S3. For all the prepared catalysts, the sorption equilibrium of TC could be reached in 30 min. As shown in Fig. 3, the adsorption capacity of the Bi_2WO_6 catalysts decreased as the pH of the hydrothermal reaction solution increased from 1 to 9. About 31% TC could be absorbed by BWO-1 while only about 11% was absorbed by BWO-9. This may be due to the relatively large S_{BET} of BWO-1 as compared to other catalysts. Thus, BWO-1 could provide more adsorption sites for TC than others. It was reported that TC could be photodegraded by superoxide radical anion ($O_2^{\bullet -}$) and singlet molecular oxygen O_2 ($^1\triangle g$) under visible light [28]. In the control experiment without any catalyst, less than 7% TC was decomposed in 300 min, suggesting that the photolysis of TC under visible light irradiation without catalyst is very weak. The photodegradation efficiency decreased as the pH of the hydrothermal reaction solution increased from 1 to 9 and BWO-1 displayed the highest degradation efficiency. Nearly 97% of TC at 20 $mg \cdot L^{-1}$ was removed in 120 min by BWO-1. To compare the photocatalytic activity of Bi_2WO_6 catalysts

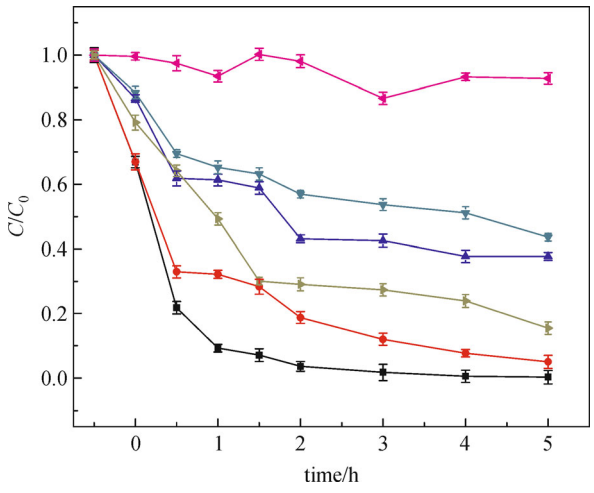

Fig. 3 Degradation kinetics of TC by Bi_2WO_6 prepared at different hydrothermal pHs under visible light irradiation. ■: pH = 1; ●: pH = 4; ▲: pH = 7; ▼: pH = 9; ►: TiO_2(P25); ◄:without catalyst

with TiO_2, the photodegradation of TC on TiO_2 was also investigated and it was found that only 71% of TC was degraded by TiO_2 in 120 min at the same conditions. At the end of reaction, the amount of TC remained on the catalysts was monitored and no TC was detected in the solids of BWO-1, suggesting that the TC adsorbed on the catalyst was completely degraded. For BWO-4, even though it had slightly smaller surface area than BWO-1, it displayed similar adsorption capacity to TC as BWO-1. However, the degradation rate of TC was only 90% in 300 min, much lower than BWO-1. Photoeletrochemical performance could be used to evaluate the efficiency of photogenerated charge interface separation for photocatalytic performance [29,30]. An on-off circulatory system was used to examine the photoresponses of ITO/Bi_2WO_6 electrodes under visible light irradiation. Figure S4 shows the results of photoelectrochemical tests of the catalysts prepared at different pHs. The photocurrent intensity generated by BWO-1 was twice of that induced by BWO-4, and -7, suggesting more efficient separation of photogenerated electron-hole pairs in BWO-1. The photocurrent generated by BWO-9 was minimal. The interface charge separation efficiency was also investigated by EIS. A smaller arc radius in the EIS Nyquist plot implies an effective separation of the photogenerated electron–hole pairs [31,32]. Figure 4(a) illustrates that the impedance arc radius of BWO-1 under visible light irradiation was smaller than in dark, indicating that there were only a few electrons across the electrolyte interface of BWO-1 without irradiation. As shown in Fig. 4(b), the arc radius of BWO-1 was the smallest among the catalysts prepared at different pHs under simulated solar light irradiation, further supporting that the photogenerated electron-hole pairs were more effectively separated in the system of BWO-1 and there was a more efficient interfacial charge transfer between the electron donor and electron acceptor [32]. This explained the high efficiency of BWO-1 to degrade TC. The degradation of TC in 300 min was 60% and 55% for BWO-7 and -9, respectively. All the reactions followed pseudo-first order kinetics and the kinetic rate constant (k) was calculated (Fig. S5). The k decreased from 1.39×10^{-2} min^{-1} for BWO-1 to 0.64, 0.21 and 0.16 $\times 10^{-2}$ min^{-1} for BWO-4, -7 and -9, respectively and it was 0.33×10^{-2} min^{-1} for TiO_2. The kinetic rate constant (k) for BWO-1 was 7 times of that for BWO-9. This result was different from that reported by Wang et al. [22], who demonstrated that the photodegradation efficiency to BPA increased as the pH of the hydrothermal reaction solution increased from 4 to 11 and the catalyst prepared at pH 11 displayed the highest degradation efficiency to BPA [22,33]. However, Amano et al. [34] reported that the photocatalytic degradation of acetic acid for Bi_2WO_6 decreased as the hydrothermal reaction solution pH increased from acid to alkaline condition. The result in the current study was in agreement with that of Chen et al. [23], who reported the catalyst prepared at pH 1 displayed the highest degradation efficiency to Microcystin-RR. Thus, the photocatalytic efficiency of Bi_2WO_6 is not only dependent on its own properties, but also on the characteristics of the reactants. In the current study, BWO-1 was used for the following experiments.

3.3 Influence of isopropanol, KI and $(NH_4)_2C_2O_4$ on the photocatalytic reaction

Isopropanol (IPA) has been used as a hydroxyl radical scavenger and KI and $(NH_4)_2C_2O_4$ as hole scavengers [33,35]. In the current study, IPA, KI and $(NH_4)_2C_2O_4$ were added in the reaction solution to illustrate the active species for the photocatalytic degradation process. As shown in Fig. 5(a), the degradation of TC by BWO-1 was slightly inhibited by IPA, and the IPA concentration (V/V) in the solution did not make big difference on the inhibition effect. This fact indicates that ·OH may not be the main reactive species responsible for the degradation of TC by Bi_2WO_6. On the contrary, the degradation was distinctly suppressed by KI and the effect increased as the concentration of KI increased (Fig. 5(b)). When the KI concentration was 10 mmol, only 70% of TC was removed after 360 min irradiation. Similarly, the inhibition effect also increased with the concentration of $(NH_4)_2C_2O_4$, and only 50% of TC was removed after 300 min irradiation when 5 mmol $(NH_4)_2C_2O_4$ was added (Fig. 5(c)). These results suggest that the photogenerated hole was mainly responsible for the degradation [36].

3.4 Photodegradation pathway

As shown Fig. 6, about 31% of total organic carbon (TOC) was removed, even though the removal rate of TC was 100% within the 360 min irradiation. This is similar with

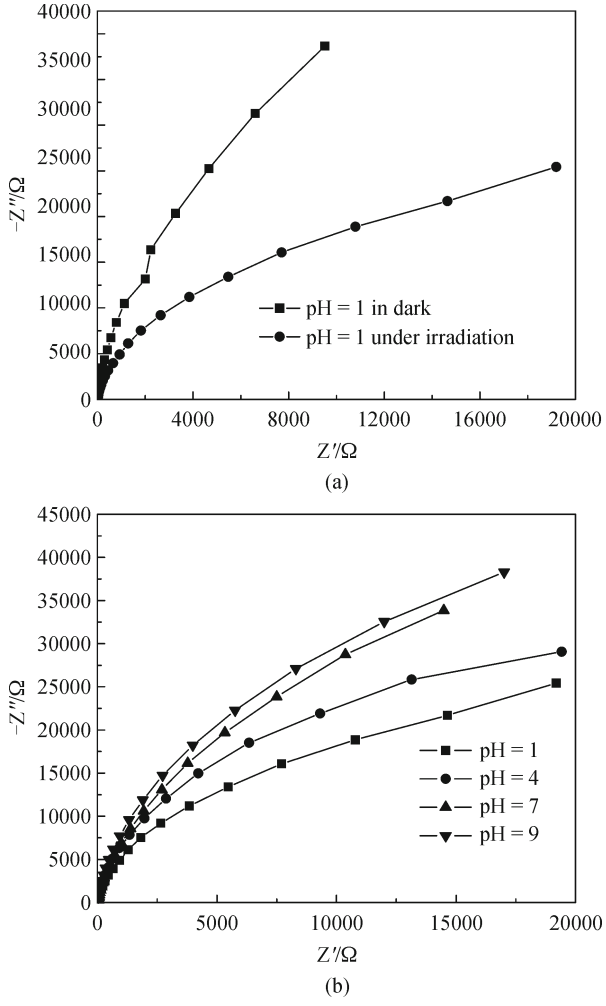

Fig. 4 Electrochemical impedance spectra (EIS) Nyquist plots of BWO-1(light *vs.* dark) (a) and EIS of different hydrothermal pHs under visible light irradiation (b)

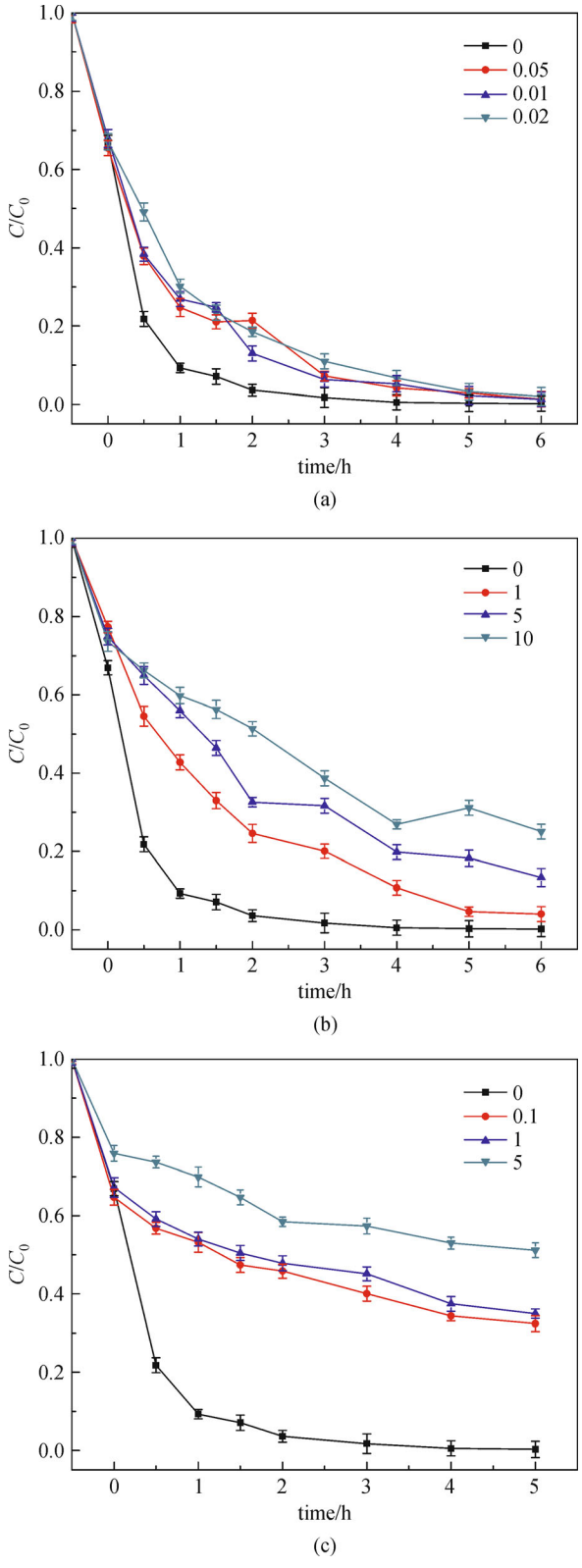

Fig. 5 The effects of isopropanol ((a), V/V), KI ((b), mmol·L^{-1}) and $(NH_4)_2C_2O_4$ ((c), mmol·L^{-1}) at different concentrations on the photodegradation of TC by BWO-1 under simulated solar light irradiation

the results reported by Hao et al. [37], who used BiOI platelet to degrade TC under visible-light for 240 min, and the TOC removal rate was only 28.68%. The results indicate that TC was mainly transformed to intermediate products but not completely mineralized. Two main intermediates were identified by LC-MS and the main fragment ions of the transformation products are shown in Table 1. Intermediate 1 with a *m/z* 400 could be a product reacted with photogenerated hole via loss of amino, *N*-methyl and hydroxyl groups [14,15,38–40]. As discussed above, photogenerated hole was the main reactive species responsible for the degradation of TC by Bi_2WO_6 [22,23]. The intermediate 2 displayed *m/z* at 477, which was proposed to occur via the reaction of ·OH at the C2-C3, C11a-C12 double-bond and a rearrangement at C12 [14,19,37,39], implying that ·OH was also involved in the degradation of TC by Bi_2WO_6 [38,40,41]. Six more intermediates with small molecular weight were detected by GC-MS and they are listed in Table S1. They were

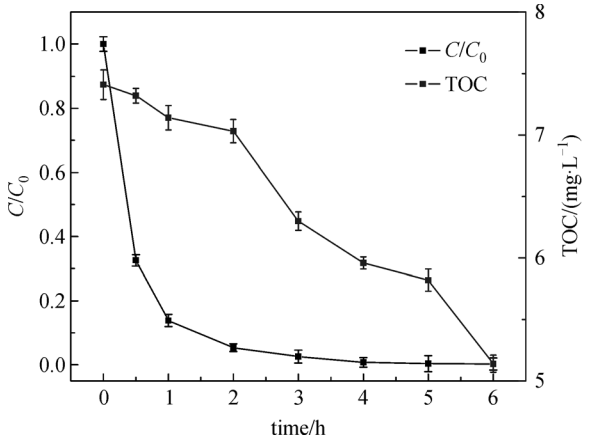

Fig. 6 Variation of TOC during photocatalytic degradation process

Table 1 Main fragment ions of TC and intermediate products

compounds	observed fragment ions at *m/z* value	
	MS	MS-MS
tetracycline	445	427, 410
intermediate 1	400	
intermediate 2	477	442

produced through the cleavage of the central carbon, and they were chemicals with one benzene ring, monoethanolamine and cyanamide. The possible degradation pathway is illustrated in Scheme 1.

4 Conclusions

Bi_2WO_6 prepared at pH 1 displayed the highest adsorption

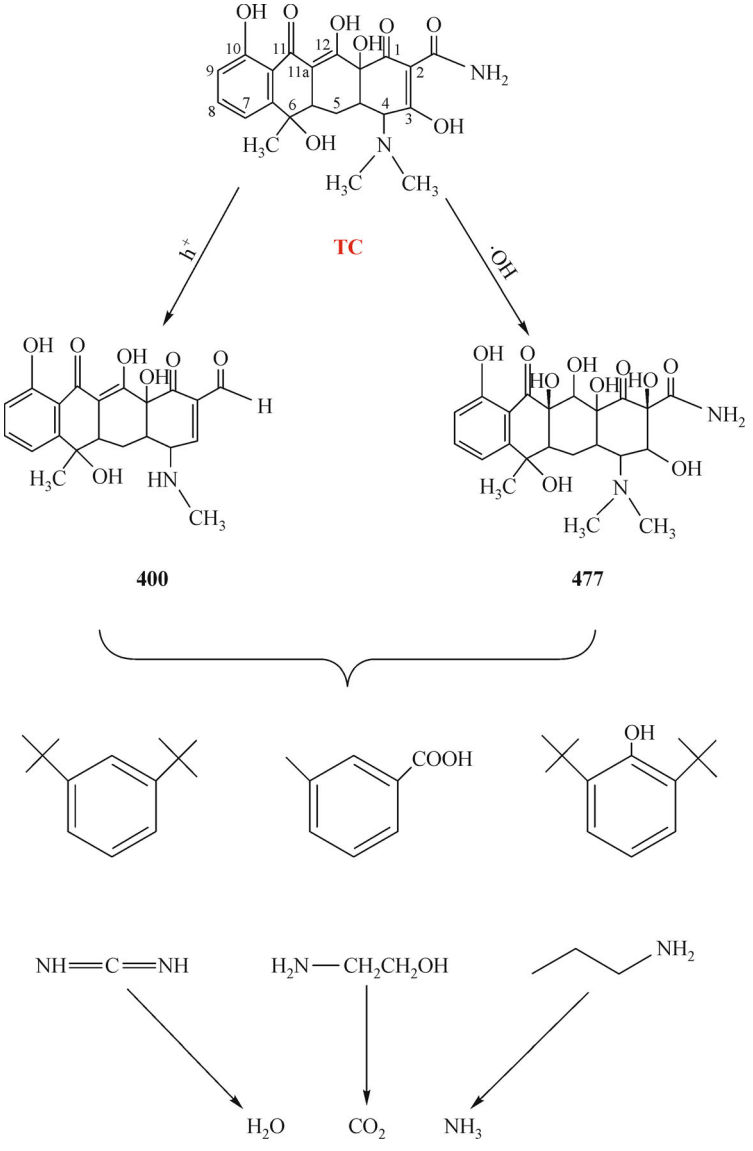

Scheme 1 Possible photocatalytic degradation pathway of TC by Bi_2WO_6

and degradation capacity to TC due to its large surface area and more efficient interfacial charge transfer between the electron donor and electron acceptor. 97% of TC at 20 mg $\cdot L^{-1}$ was removed by 0.5 g $\cdot L^{-1}$ of Bi_2WO_6 solids after 120 min irradiation of simulated solar light. Photogenerated holes were suggested as the main active species responsible for the degradation of TC and the produced $\cdot OH$ was also involved in the reaction. Due to the intermediates produced during the reaction, only 31% TOC was removed in 360 min irradiation, at which TC was completely degraded.

Acknowledgements This research was supported by Ministry of Science and Technology of China (Grant Nos: 2014CB932001 and 2012ZX07529-003), Tianjin Municipal Science and Technology Commission (13JCZDJC35900), and the Ministry of Education innovation team (IRT 13024).

Supporting information is available in the online version of this article at http://dx.doi.org/10.1007/s11783-014-0753-y and is accessible for authorized users.

References

1. Khetan S K, Collins T J, Human pharmaceuticals in the aquatic environment: a challenge to Green Chemistry. Chemical Reviews, 2007, 107(6): 2319–2364
2. Stuer-Lauridsen F, Birkved M, Hansen L P, Lützhøft H C H, Halling-Sørensen B. Environmental risk assessment of human pharmaceuticals in Denmark after normal therapeutic use. Chemosphere, 2000, 41(9): 1509–1509
3. Wang D, Li Y, Li G, Wang C, Zhang W, Wang Q. Development and modeling of a flat plate serpentine reactor for photocatalytic degradation of 17-ethinylestradiol. Environmental Science and Pollution Research International, 2013, 20(4): 2321–2329
4. Wang D, Li Y, Li G, Wang C, Zhang W, Wang Q. Modeling of quantitative effects of water components on the photocatalytic degradation of 17α-ethynylestradiol in a modified flat plate serpentine reactor. Journal of Hazardous Materials, 2013, 254–255: 64–71
5. Bautitz I R, Nogueira R F P. Degradation of tetracycline by photo-Fenton process -Solar irradiation and matrix effects. Journal of Photochemistry and Photobiology A: Chemistry, 2007, 187(1,5): 33–39
6. Karthikeyan K G, Meyer M T. Occurrence of antibiotics in wastewater treatment facilities in Wisconsin, USA. Science of the Total Environment, 2006, 361(1–3): 196–207
7. Kolpin D W, Furlong E T, Meyer M T, Thurman E M, Zaugg S D, Barber L B, Buxton H T. Pharmaceuticals, hormones, and other organic wastewater contaminants in U.S. streams, 1999–2000: a national reconnaissance. Environmental Science & Technology, 2002, 36(6): 1202–1211
8. Stumpf M, Ternes T A, Wilken R D, Rodrigues S V, Baumann W. Polar drug residues in sewage and natural waters in the state of Rio de Janeiro, Brazil. Science of the Total Environment, 1999, 225(1–2): 135–141
9. Kümmerer K. Antibiotics in the aquatic environment: a review—Part I. Chemosphere, 2009, 75(4): 417–434
10. Pailler J Y, Krein A, Pfister L, Hoffmann L, Guignard C. Solid phase extraction coupled to liquid chromatography-tandem mass spectrometry analysis of sulfonamides, tetracyclines, analgesics and hormones in surface water and wastewater in Luxembourg. Science of the Total Environment, 2009, 407(16): 4736–4743
11. Khan M H, Bae H, Jung J Y. Tetracycline degradation by ozonation in the aqueous phase: proposed degradation intermediates and pathway. Journal of Hazardous Materials, 2010, 181(1–3): 659–665
12. Liu S, Zhao X R, Sun H Y, Li R R, Fang Y F, Huang Y P. The degradation of tetracycline in a photo-electro-Fenton system. Chemical Engineering Journal, 2013, 231: 441–448
13. Gómez-Pacheco C V, Sánchez-Polo M, Rivera-Utrilla J, López-Peñalver J J. Tetracycline degradation in aqueous phase by ultraviolet radiation. Chemical Engineering Journal, 2012, 187(1): 89–95
14. Zhu X D, Wang Y J, Sun R J, Zhou D M. Photocatalytic degradation of tetracycline in aqueous solution by nanosized TiO_2. Chemosphere, 2013, 92(8): 925–932
15. Wang P, Yap P S, Lim T T. C–N–S tridoped TiO_2 for photocatalytic degradation of tetracycline under visible-light irradiation. Applied Catalysis A: General, 2011, 399(1–2): 252–261
16. Wang D, Li Y, Li G, Wang C, Wang P, Zhang W, Wang Q. Ag/AgCl@helical chiral TiO_2 nanofibers as a visible-light driven plasmon photocatalyst. Chemical Communications, 2013, 49(88): 10367–10369
17. Li Y Y, Liu J P, Huang X T, Li G Y. Hydrothermal synthesis of Bi_2WO_6 uniform hierarchical microspheres. Crystal Growth & Design, 2007, 7(7): 1350–1355
18. Shang M, Wang W Z, Sun S M, Zhou L, Zhang L. Bi_2WO_6 nanocrystals with high photocatalytic activities under visible light. Journal of Physical Chemistry C, 2008, 112(28): 10407–10411
19. Dai K, Peng T Y, Chen H, Liu J, Zan L. Photocatalytic degradation of commercial phoxim over La-doped TiO_2 nanoparticles in aqueous suspension. Environmental Science & Technology, 2009, 43(5): 1540–1545
20. Shang M, Wang W Z, Sun S M, Ren J, Zhou L, Zhang L. Efficient visible light-induced photocatalytic degradation of contaminant by spindle-like PANI/$BiVO_4$. Journal of Physical Chemistry C, 2009, 113(47): 20228–20233
21. Kudo A, Hijii S. H_2 or O_2 evolution from aqueous solutions on layered oxide photocatalysts consisting of Bi^{3+} with $6s^2$ configuration and d0 transition metal ions. Chemistry Letters, 1999, 28(10): 1103–1104
22. Wang C, Zhang H, Li F, Zhu L. Degradation and mineralization of bisphenol A by mesoporous Bi_2WO_6 under simulated solar light irradiation. Environmental Science & Technology, 2010, 44(17): 6843–6848
23. Chen P, Zhu L, Fang S, Wang C, Shan G. Photocatalytic degradation efficiency and mechanism of microcystin-RR by mesoporous Bi_2WO_6 under near ultraviolet light. Environmental Science & Technology, 2012, 46(4): 2345–2351
24. Nyholm R, Berndtsson A, Martensson N. Core level binding energies for the elements Hf to Bi ($Z = 72 – 83$). Journal of Physics C: Solid State Physics, 1980, 13(36): 1091–1096
25. Yao S S, Wei J Y, Huang B B, Feng S Y, Zhang X Y, Qin X Y,

Wang P, Wang Z Y, Zhang Q, Jing X Y, Zhan J. Morphology modulated growth of bismuth tungsten oxide nanocrystals. Journal of Solid State Chemistry, 2009, 182(2): 236–239

26. Pierotti R, Rouquerol J. Reporting physisorption data for gas/solid systems with special reference to the determination of surface area and porosity. Pure and Applied Chemistry, 1985, 57: 603–619
27. Huang Y, Ai Z, Ho W, Chen M, Lee S. Ultrasonic spray pyrolysis synthesis of porous Bi_2WO_6 microspheres and their visible-light-induced photocatalytic removal of NO. Journal of Physics and Chemistry C, 2010, 114(14): 6342–6349
28. Castillo C, Criado S, Díaz M, García N A. Riboflavin as a sensitiser in the photodegradation of tetracyclines. Kinetics, mechanism and microbiological implications. Dyes and Pigments, 2007, 72(2): 178–184
29. Chang C, Fu Y, Hu M, Wang C, Shan G, Zhu L. Photodegradation of bisphenol A by highly stable palladium-doped mesoporous graphite carbon nitride (Pd/mpg-C_3N_4) under simulated solar light irradiation. Applied Catalysis B: Environmental, 2013, 142–143: 553–560
30. Wang X, Chen X, Thomas A, Fu X, Antonietti M. Metal-containing carbon nitride compounds: a new functional organic–metal hybrid material. Advanced Materials, 2009, 21(16): 1609–1612
31. Xiao F, Wang F, Fu X, Zheng Y. A green and facile self-assembly preparation of gold nanoparticles/ZnO nanocomposite for photocatalytic and photoelectrochemical applications. Journal of Materials Chemistry, 2012, 22(7): 2868–2877
32. Zhang Y, Zhang N, Tang Z R, Xu Y J. Transforming C_dS into an efficient visible light photocatalyst for selective oxidation of saturated primary C-H bonds under ambient conditions. Chemical Science, 2012, 3: 2812–2822
33. Wang C, Zhu L, Wei M, Chen P, Shan G. Photolytic reaction mechanism and impacts of coexisting substances on photodegradation of bisphenol A by Bi_2WO_6 in water. Water Research, 2012, 46 (3): 845–853
34. Amano F, Nogami K, Ohtani B. Enhanced photocatalytic activity of bismuth-tungsten mixed oxides for oxidative decomposition of acetaldehyde under visible light irradiation. Catalysis Communications, 2012, 20(5): 12–16
35. Ng J, Wang X, Sun D D. One-pot hydrothermal synthesis of a hierarchical nanofungus-like anatase TiO_2 thin film for photocatalytic oxidation of bisphenol A. Applied Catalysis B: Environmental, 2011, 110(2): 260–272
36. Wang R C, Ren D J, Xia S Q, Zhang Y L, Zhao J F. Photocatalytic degradation of Bisphenol A (BPA) using immobilized TiO_2 and UV illumination in a horizontal circulating bed photocatalytic reactor (HCBPR). Journal of Hazardous Materials, 2009, 169(1–3): 926–932
37. Hao R, Xiao X, Zuo X X, Nan J M, Zhang W D. Efficient adsorption and visible-light photocatalytic degradation of tetracycline hydrochloride using mesoporous BiOI microspheres. Journal of Hazardous Materials, 2012, 209-210(30): 137–145
38. Yuan F, Hu C, Hu X X, Wei D B, Chen Y, Qu J H. Photodegradation and toxicity changes of antibiotics in UV and UV/H_2O_2 process. Journal of Hazardous Materials, 2011, 185(2–3): 1256–1263
39. Dai K, Peng T Y, Chen H, Zhang R X, Zhang Y X. Photocatalytic degradation and mineralization of commercial methamidophos in aqueous titania suspension. Environmental Science & Technology, 2008, 42(5): 1505–1510
40. Wang Y, Zhang H, Chen L, Wang S, Zhang D. Ozonation combined with ultrasound for the degradation of tetracycline in a rectangular air-lift reactor. Separation and Purification Technology, 2012, 84(9): 138–146
41. Wang Y, Zhang H, Zhang J, Lu C, Huang Q, Wu J, Liu F. Degradation of tetracycline in aqueous media by ozonation in an internal loop-lift reactor. Journal of Hazardous Materials, 2011, 192 (1): 35–43